Cellular/Molecular

# Differential Ubiquitination and Proteasome Regulation of $Ca_V2.2$ N-Type Channel Splice Isoforms

**Spiro Marangoudakis, Arturo Andrade, Thomas D. Helton, Sylvia Denome, Andrew J. Castiglioni, and Diane Lipscombe**

Department of Neuroscience, Brown University, Providence, Rhode Island 02912

**$Ca_V2.2$ (N-type) calcium channels control the entry of calcium into neurons to regulate essential functions but most notably presynaptic transmitter release. $Ca_V2.2$ channel expression levels are precisely controlled, but we know little of the cellular mechanisms involved. The ubiquitin proteasome system (UPS) is known to regulate expression of many synaptic proteins, including presynaptic elements, to optimize synaptic efficiency. However, we have limited information about ubiquitination of $Ca_V2$ channels. Here we show that $Ca_V2.2$ proteins are ubiquitinated, and that elements in the proximal C terminus of $Ca_V2.2$ encoded by exon 37b of the mouse *Cacna1b* gene predispose cloned and native channels to downregulation by the UPS. $Ca_V2.2$ channels containing e37b are expressed throughout the mammalian nervous system, but in some cells, notably nociceptors, sometimes e37a—not e37b—is selected during alternative splicing of $Ca_V2.2$ pre-mRNA. By a combination of biochemical and functional analyses we show e37b promotes a form of ubiquitination that is coupled to reduced $Ca_V2.2$ current density and increased sensitivity to the UPS. Cell-specific alternative splicing of e37a in nociceptors reduces $Ca_V2.2$ channel ubiquitination and sensitivity to the UPS, suggesting a role in pain processing.**

## Introduction

Presynaptic $Ca_V2$ channels mediate calcium entry to trigger neurotransmitter release and support synaptic transmission (Catterall, 2000). $Ca_V2.2$ proteins are the main component of N-type currents. They are sensitive to regulation by several cellular mechanisms with distinct temporal characteristics, including G-protein-coupled receptors, posttranslational modifications, and protein interactions (Dunlap and Fischbach, 1978; Holz et al., 1986; Hille et al., 1995; Ikeda and Dunlap, 1999; Dolphin, 2003). Relative to other synaptic proteins particularly postsynaptic receptors (Chen and Roche, 2007; Yi and Ehlers, 2007), we know little about the cellular mechanisms that control surface expression of presynaptic $Ca_V2.2$ channels.

Ubiquitination influences synaptic efficiency by modifying the trafficking, endocytosis and activity of synaptic receptors and ion channels (Colledge et al., 2003; Patrick et al., 2003; DiAntonio and Hicke, 2004; Yi and Ehlers, 2007; Altier et al., 2011; Rotin and Staub, 2011). Despite functional evidence that ubiquitin-dependent changes in synaptic efficacy involve presynaptic components (Speese et al., 2003; Bingol and Schuman, 2005; Rinetti and Schweizer, 2010), $Ca_V2$ channels were only recently recognized as targets of the ubiquitin proteasome system (UPS) (Waithe et al., 2011).

Neurons employ alternative pre-mRNA splicing to optimize $Ca_V2.2$ channel activity (Lipscombe, 2005; Liao and Soong, 2010). By comparing the properties of functionally validated splice isoforms we, and others, have revealed critical structural domains in $Ca_V2.2$ channels that control channel activity and modulation by signaling molecules (Maximov and Bezprozvanny, 2002; Bell et al., 2004; Altier et al., 2007; Raingo et al., 2007). One site of alternative splicing in $Ca_V2.2$ involves a pair of mutually exclusive exons, e37a and e37b. Each exon encodes a 33 aa sequence of the proximal C terminus of the $Ca_V2.2$ channel; the two sequences differ by 14 aa (Fig. 1*A*; Bell et al., 2004). $Ca_V2.2$-e37a channels are enriched in nociceptors of dorsal root ganglia, and they are associated with relatively large $Ca_V2.2$ current densities and greater susceptibility to voltage-independent inhibition by certain $G_{i/o}$ protein-coupled receptors ($G_{i/o}$PCR). By contrast, $Ca_V2.2$-e37b channels are expressed widely throughout the nervous system, are associated with smaller current densities, and are less susceptible to $G_{i/o}$PCR inhibition (Bell et al., 2004; Castiglioni et al., 2006; Raingo et al., 2007; Andrade et al., 2010). By comparing $Ca_V2.2$ gating currents in cells expressing $Ca_V2.2$-e37a and $Ca_V2.2$-e37b clones, we showed selection of e37a over e37b was associated with significantly more functional channels at the cell surface (Castiglioni et al., 2006). A partially overlapping homologous region of postsynaptic $Ca_V1.2$ channels was recently shown to regulate channel density at the plasma membrane (Altier et al., 2011). In this study Zamponi and colleagues also linked $Ca_V1.2$ expression levels to ubiquitination (Altier et al., 2011).

Received Feb. 7, 2011; revised May 4, 2012; accepted May 31, 2012.

Author contributions: S.M., A.A., T.D.H., and D.L. designed research; S.M., A.A., T.D.H., S.D., and A.J.C. performed research; S.M., A.A., T.D.H., and D.L. analyzed data; S.M., A.A., A.J.C., and D.L. wrote the paper.

This work was supported by NIH Grants NS29967, NS055251 (D.L.), and 1F31NS066702 (S.M.) and funds from Consejo Nacional de Ciencia y Tecnología, Mexico (A.A.). We thank Dr. Pietro De Camilli (Yale University) for the HA-Ub clone. We appreciate discussions with Drs. Jeffrey Singer and Jeffrey Laney. S.M. was a graduate student in the Molecular Biology, Cell Biology and Biochemistry Program at Brown University.

The authors declare no competing financial interests.

Correspondence should be addressed to Dr. Diane Lipscombe, Department of Neuroscience, Brown University, 185 Meeting Street, Providence, RI 02912. E-mail: Diane_Lipscombe@Brown.edu.

T. D. Helton's current address: Pfizer Inc., Neuroscience, Cambridge, MA 02138.

A. J. Castiglioni's current address: Argonne National Laboratory, Nuclear Engineering Division, 9700 South Class Avenue, Argonne, IL 60439.

DOI:10.1523/JNEUROSCI.0851-11.2012

 0270-6474/12/3210365-05$15.00/0

We postulated that ubiquitination and regulation by the UPS might underlie functional differences in current densities between e37 splice isoforms of $Ca_V2.2$. We show e37b-specific ubiquitination of $Ca_V2.2$ protein that is absent in e37a channels and that e37b-specific ubiquitination is linked to greater sensitivity of channels to the UPS. Cell-specific alternative splicing to enrich for e37a-containing channels reduces $Ca_V2.2$ ubiquitination and sensitivity to the UPS.

## Materials and Methods

*Molecular biology and cloning.* Construction of full-length calcium channel clones and accessory subunits were described previously (Raingo et al., 2007). The hemagglutinin (HA)-tagged ubiquitin (Ub) HA-Ub clone (in pcDNA3) was a generous gift from Pietro De Camilli (Yale University, New Haven CT).

*Immunoprecipitation and Western blot analyses.* Calcium channel $\alpha_1$ subunits $Ca_V2.2$-e37a or $Ca_V2.2$-e37b together with $Ca_V\beta_3$, $Ca_V\alpha_2\delta_1$, and eGFP were expressed transiently in tsA201 cells as described previously (Raingo et al., 2007), with HA-Ub cDNAs. We harvested cells 24 h after transfection. For immunoprecipitations (IPs), ~1 mg of total protein lysates were incubated at 4°C overnight with 2 $\mu$g of polyclonal anti-$Ca_V2.2$ and 100 $\mu$l of protein A agarose slurry (Sigma, catalog #P3476). Westerns were performed as described previously (Andrade et al., 2010). Primary antibodies were: rabbit anti-$Ca_V2.2$ polyclonal (1:200; Alomone, catalog #ACC-002), mouse anti-ubiquitin monoclonal (1:200; Cell Signaling Technology, P4D1), and HRP-conjugated rat anti-HA monoclonal antibodies (1:7500; Roche, clone 3F10). HRP-labeled donkey $\alpha$-rabbit and $\alpha$-mouse IgG (Jackson ImmunoResearch catalog #711-036-152 and #715-035-151, respectively) were used at ≥1:10,000 dilution. Further details are provided in (Andrade et al., 2010). We demonstrated antibody specificity by several experiments including (1) the precise overlap of anti-HA-Ub and anti-Ub signals establishing that antibodies to HA and to Ub recognize the same protein pool (Fig. 1*C*); (2) the complete absence of anti-HA-Ub signal in protein samples from cells lacking $Ca_V2.2$ following immunoprecipitation with anti-$Ca_V2.2$—despite strong ubiquitination of total protein in lysate (lanes 3 in lysate and after $Ca_V2.2$ IP; Fig. 1*D*); and (3) the absence of anti-$Ca_V2.2$ signal in cells lacking $Ca_V2.2$.

*Electrophysiology.* Calcium currents were recorded from tsA201 cells and acutely isolated nociceptors of dorsal root ganglia (P6–P9 mice of both sexes) using standard whole-cell patch-clamp methods as described previously (Raingo et al., 2007, Andrade et al., 2010). The external solution contained 1 mM $CaCl_2$ as charge carrier. The pipette solution contained (in mM) 126 CsCl, 10 EGTA, 1 EDTA, 10 HEPES, 4 MgATP, pH 7.2 with CsOH. Cells were maintained in standard growth medium (DMEM + 10% FBS) supplemented with 5 $\mu$M MG132 in 0.1% DMSO or 0.1% DMSO alone for control 1–3 h before recording. In neurons, $\omega$-conotoxin GVIA subtraction and capsaicin screening were performed as described previously (Andrade et al., 2010). All recordings were performed at room temperature.

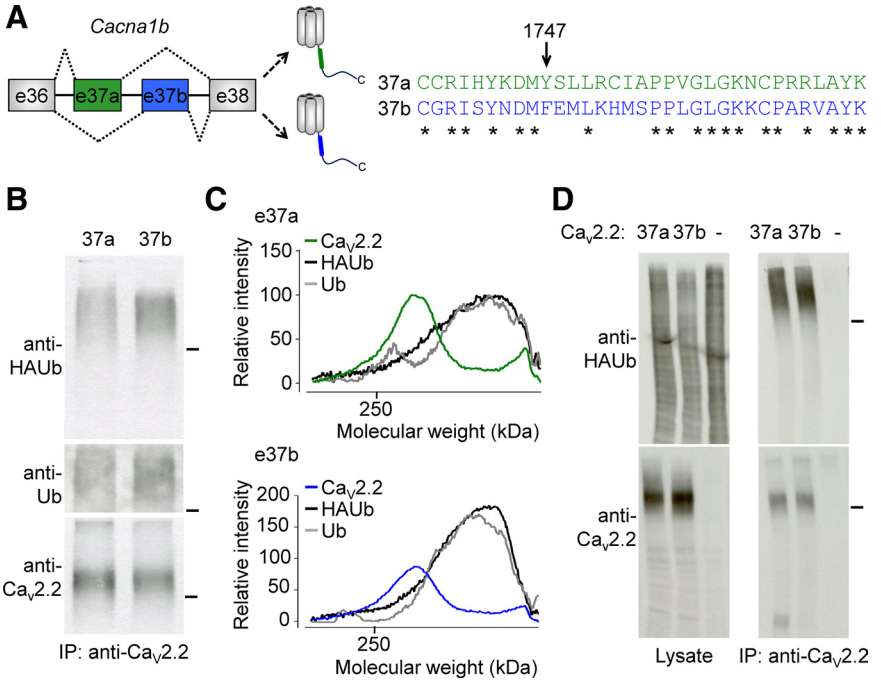


**Figure 1.** Alternatively spliced exons e37a and e37b influence ubiquitination of $Ca_V2.2$ channels. ***A***, Left, Pattern of mutually exclusive alternative splicing of e37a and e37b in the $Ca_V2.2$ encoding gene, *Cacna1b*. Right, Amino acid sequences of e37a and e37b aligned; asterisks denote 19 aa conserved between exons. Arrow highlights critical Y1747 in e37a and F1747 in e37b. ***B–D***, Western blots compare levels of ubiquitin associated with e37a-$Ca_V2.2$ and 37b-$Ca_V2.2$ protein isolated from tsA201 cells. Cells were transfected with cDNAs for HA-Ub, $Ca_V\beta_3$, and e37a-$Ca_V2.2$ (37a) or e37b-$Ca_V2.2$ (37b). ***B***, Protein immunoprecipitated with antibodies to $Ca_V2.2$, same membrane probed with anti-HA-Ub (top) then sequentially stripped and reprobed with anti-Ub (middle), and anti-$Ca_V2.2$ (bottom). Black bar is the 250 kDa marker. ***C***, Relative signal intensities for e37a (top) and e37b (bottom) signals plotted according to migration into the gel and referenced to the 250 kDa marker. Image density analyzed with ImageJ software. Signal intensities were normalized to the peak of e37a signal for comparison. ***D***, Western blots of protein lysate (left) and immunoprecipitated using $Ca_V2.2$ antibody (right) from tsA201 cells transfected with e37a-$Ca_V2.2$, e37b-$Ca_V2.2$, or empty vector (−). Membrane probed with anti-HA-Ub (top) and stripped and reprobed with anti-$Ca_V2.2$ (bottom) illustrates the specificity of both HA-Ub and $Ca_V2.2$ antibodies.

## Results

$Ca_V2.2$-e37a and $Ca_V2.2$-e37b channels only differ in 14 aa (Fig. 1*A*), but these few changes result in functional differences in current density and G-protein modulation. We expressed full-length $Ca_V2.2$-e37a and $Ca_V2.2$-e37b channel isoforms in tsA201 cells, a system we used previously to characterize their different properties. HA-Ub allowed us to monitor Ub levels with high specificity using anti-HA, following immunoprecipitation with anti-$Ca_V2.2$ (Figs. 1–3). We showed HA-Ub signals were associated with both $Ca_V2.2$ isoforms, but Ub levels associated with $Ca_V2.2$-e37b were consistently greater compared with $Ca_V2.2$-e37a (Figs. 1–3).

We compared the migration of $Ca_V2.2$ and Ub-$Ca_V2.2$ signals in the same protein gel by stripping the same membrane and reprobing using different antibodies. Migrations of the major anti-Ub and anti-HA-Ub signals were impeded relative to the major $Ca_V2.2$ signal located just above the 250 kDa marker (Fig. 1*B*,*C*), consistent with higher molecular masses of ubiquitinated protein. The anti-$Ca_V2.2$ signal is above background over the range encompassing Ub-$Ca_V2.2$ (Fig. 1*C*) although the major pool of immunoprecipitated $Ca_V2.2$ protein does not appear to be ubiquitinated. Similar data have been published previously (Altier et al., 2011; Waithe et al., 2011, see their supplemental data). We quantified Ub-$Ca_V2.2$ signals and found $Ca_V2.2$-e37b protein was associated with ~70% greater ubiquitination compared with $Ca_V2.2$-e37a for the same level of total $Ca_V2.2$ protein (Student's *t* test, $p = 0.017$; Fig. 2*A*,*B*). E37b-dependent ubiquitination is consistent with the lower current densities of $Ca_V2.2$-e37b isoforms compared with $Ca_V2.2$-e37a (Castiglioni et al., 2006).

In a previous study, we identified an amino acid unique to e37a, Y1747 (F1747 in e37b), critical for supporting the major functional differences between $Ca_V2.2$ isoforms (Fig. 1*A*; Raingo et al., 2007). We showed that replacing Y1747 with F1747 in $Ca_V2.2$-e37a

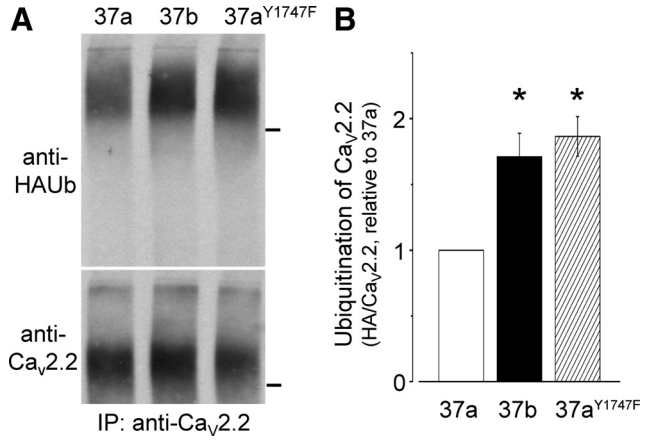


**Figure 2.** Tyrosine 1747 in e37a is critical for reduced ubiquitination of e37a-$Ca_V2.2$ channels compared with e37b-$Ca_V2.2$. ***A***, Western blots compare ubiquitin associated with e37a, e37b, and e37a$^{Y1747F}$ $Ca_V2.2$ channels expressed in tsA201 cells. Anti-HA-Ub signals (top) and anti-$Ca_V2.2$ signals (bottom) from the same membrane blots stripped and reprobed. Black bar is the 250 kDa marker. ***B***, Average intensity of anti-HA-Ub signal normalized to anti-$Ca_V2.2$ signal for each experiment. Values are plotted relative to the e37a-$Ca_V2.2$ signal for comparison. Values plotted are means ± SEM. E37b and e37a$^{Y1747F}$ averages are significantly >1; *p* values were: $p = 0.017$ ($n = 3$) and $p = 0.005$ ($n = 3$).

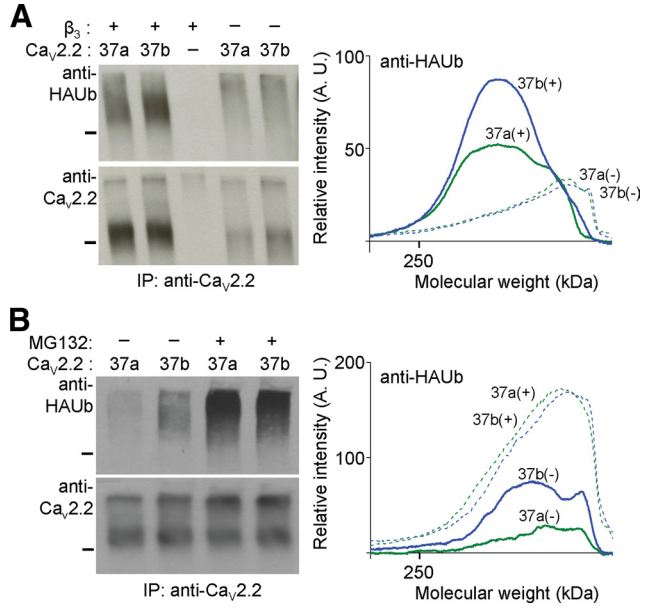


**Figure 3.** Effects of $Ca_V\beta_3$ subunit and of inhibiting the proteasome using MG132 on ubiquitination of $Ca_V2.2$. ***A***, Anti-HA-Ub signals for e37a and e37b $Ca_V2.2$ protein isoforms isolated from tsA201 cells transfected with (lanes 1–3; solid lines) and without (lanes 4–5; dashed lines) $Ca_V\beta_3$. Cells expressing $Ca_V\beta_3$ but lacking $Ca_V2.2$ (empty vector) illustrates the specificity of antibodies (lane 3). ***B***, Anti-HA-Ub signals for $Ca_V2.2$ protein isoforms under control conditions (solid lines) and after incubation with 10 $\mu$M MG132 (dashed lines). ***A***, ***B***, Left, Protein immunoprecipitated with antibodies to $Ca_V2.2$, same membranes probed with anti-HA-Ub (top), then stripped and reprobed with anti-Ub anti-$Ca_V2.2$ (bottom). Black bars are 250 kDa markers. Intensities for e37a (top) and e37b (bottom) signals plotted according to migration into the gel and referenced to the 250 kDa marker. Image density analyzed with ImageJ software (Abramoff et al., 2004).

($Ca_V2.2$-e37a$^{Y1747F}$) reduced current densities to levels indistinguishable from $Ca_V2.2$-e37b (Raingo et al., 2007). We used this single point mutant of $Ca_V2.2$-e37a to test whether lower current density is associated with increased ubiquitination. We measured Ub-$Ca_V2.2$-e37a$^{Y1747F}$ levels in tsA201 cells and compared with wild-type channels. We found that the Ub signal associated with immunoprecipitated $Ca_V2.2$-e37a$^{Y1747F}$ protein was significantly greater than wild-type $Ca_V2.2$-e37a (Student's test, $p = 0.005$) and statistically indistinguishable from that of $Ca_V2.2$-e37b (Student's *t* test, $p = 0.54$; Fig. 2*A*,*B*). These data further support a link between e37b-dependent ubiquitination, functional channels, and reduced $Ca_V2.2$ current densities (Raingo et al., 2007).

$Ca_V\beta$ subunits are required for surface expression of $Ca_V1$ and $Ca_V2$ channels (Leroy et al., 2005) and are proposed to protect $Ca_V1$ and $Ca_V2$ channels from degradation by the UPS (Altier et al., 2011; Waithe et al., 2011). We tested whether $Ca_V\beta_3$ subunits affect ubiquitination of $Ca_V2.2$. In the absence of $Ca_V\beta_3$, we found that both anti-$Ca_V2.2$ and anti-HA-Ub signals are reduced. This is thought to reflect increased rates of degradation of $Ca_V\beta_3$-less $Ca_V2.2$ protein that does not reach the plasma membrane (Waithe et al., 2011). Migration of the Ub-$Ca_V2.2$ protein pool from cells lacking $Ca_V\beta_3$ was also impeded relative to protein from control cells (Fig. 3*A*). In the absence of $Ca_V\beta_3$, Ub signals associated with e37a and 37b isoforms were not different. Therefore, our data suggest that e37b-dependent ubiquitination is observed when $Ca_V\beta_3$ subunits are coexpressed and when functional $Ca_V2.2$ channels are expressed on the cell surface.

Next we tested whether e37b-depedent ubiquitinated $Ca_V2.2$ protein is susceptible to degradation through the UPS. We used MG132 to inhibit the UPS and compared e37a and e37b associated Ub signals (Bloom and Pagano, 2005). As shown by others, in the presence of $Ca_V\beta_3$, MG132 did not lead to an increase in bulk $Ca_V2.2$ protein levels (Waithe et al., 2011; see Altier et al., 2011 for studies on $Ca_V1.2$; Kim et al., 2011). We did observe a substantial increase in Ub-$Ca_V2.2$ signal intensities of both isoforms consistent with build up of ubiquitinated protein after blocking the proteasome with MG132, but under these conditions, isoform-specific differences in ubiquitination between e37a and e37b channels were lost (Fig. 3*B*). Although we show that both isoforms are sensitive to the UPS, this experiment does not give insight into the functional consequences of proteasome inhibition, or allow us to establish which pool of ubiquitinated protein is targeted to the UPS.

We therefore assessed the consequences of UPS inhibition on functional $Ca_V2.2$ channels, and compared current densities in tsA201 cells expressing $Ca_V2.2$-e37a and $Ca_V2.2$-e37b isoforms before and after treatment with MG132. $Ca_V2.2$ current densities in tsA201 cells expressing $Ca_V2.2$-e37a are significantly larger than those in cells expressing $Ca_V2.2$-e37b (Bell et al., 2004; Castiglioni et al., 2006; Raingo et al., 2007; Fig. 4*A*,*B*). Peak $Ca_V2.2$ current densities in cells expressing $Ca_V2.2$-e37a were slightly although not significantly increased following MG132 treatment (Student's *t* test, $p = 0.10$), by contrast $Ca_V2.2$ current densities in cells expressing $Ca_V2.2$-e37b increased by almost 50% relative to control (Student's *t* test, $p = 0.016$; Fig. 4*A*,*B*). These experiments suggest that e37b-specific ubiquitinated $Ca_V2.2$ proteins are downregulated by the UPS influencing the density of functional $Ca_V2.2$ channels on the cell surface. It is also interesting that the difference in $Ca_V2.2$ current densities between isoforms is normalized when the UPS is inhibited (Fig. 4*A*,*B*).

Finally, we assessed the effect of UPS inhibition on native $Ca_V2.2$ currents in neurons (Fig. 4*C–F*). Although we lack antibodies to discriminate between $Ca_V2.2$ isoforms, we have mice that only expressed e37b-$Ca_V2.2$ channels to compare to wild-type that express both e37a and e37b isoforms. We generated the e37b-only mouse line by replacing e37a with e37b and creating a *Cacna1b* gene contained two e37b sequences (*Cacna1b*$^{b*b/b*b}$; Andrade et al., 2010). Nociceptors of dorsal root ganglia normally express both e37a and e37b isoforms (Bell et al., 2004). Therefore, we compared the actions of MG132 on $Ca_V2.2$ currents in nociceptors of wild-type mice (e37a + e37b) to those from mice that express a second copy of e37b

instead of e37a (e37b* + e37b). We isolated $Ca_V2.2$ currents in nociceptors from all other calcium currents with the highly selective $Ca_V2.2$ inhibitor, ω-conotoxin GIVA (Andrade et al., 2010). This allowed us to separate the effects of MG132 on $Ca_V2.2$ (toxin-sensitive) from non-$Ca_V2.2$ (toxin-insensitive) channels. $Ca_V2.2$ currents in nociceptors of e37b-only mice increased 41% after MG132 compared with control ($p = 0.0013$; Fig. 4*D*), by contrast, $Ca_V2.2$ currents in nociceptors of wild-type mice that normally express e37a-containing channels were not significantly different from control currents when treated with MG132 ($p = 0.32$; Fig. 4*C*). MG132 enhanced non-$Ca_V2.2$ currents (toxin-insensitive) in nociceptors of WT mice (58%; $p = 0.03$) and e37b-only mice (54%; $p = 0.03$) by the same extent (Fig. 4*E*,*F*). Our data show that e37b-$Ca_V2.2$ channels, as well as non-$Ca_V2.2$ channels (toxin-insensitive), are susceptible to downregulation by the UPS in contrast to e37a-$Ca_V2.2$ channels that are relatively insensitive to UPS inhibition.

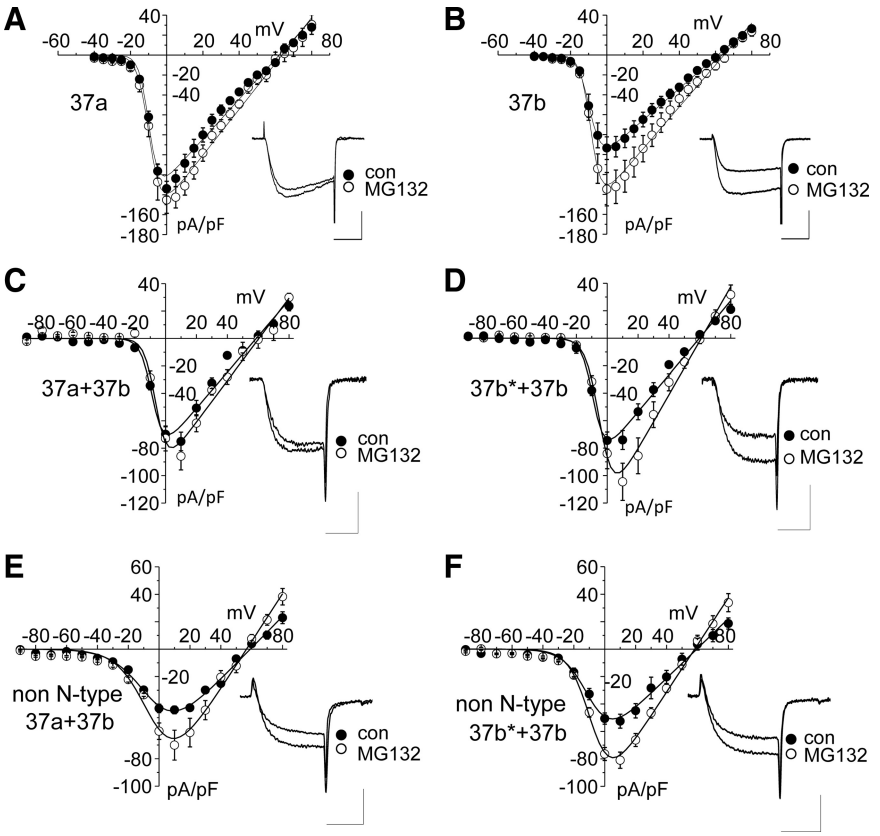


**Figure 4.** Inhibition of the proteasome increases $Ca_V2.2$ current densities in tsA201 cells expressing e37b clones and in nociceptors from mice that express only e37b-$Ca_V2.2$ not e37a-$Ca_V2.2$ isoforms. ***A***, ***B***, *I–V* relationships for $Ca_V2.2$ currents in tsA201 cells expressing recombinant e37a (***A***) and e37b (***B***) $Ca_V2.2$ channels in control (solid circles) and after 3 h treatment with 5 μM MG132 (open circles). ***A***, Peak average e37a currents in control were −133.9 ± 7.4 pA/pF, $n = 10$, and 145.2 ± 13.4 pA/pF, $n = 11$, after MG132 (Student's *t* test, $p = 0.10$). ***B***, Peak average e37b currents in control were −93.5 ± 11.3 pA/pF, $n = 11$, and −134.7 ± 16.8 pA/pF, $n = 11$, after MG132 treatment (Student's *t* test; $p = 0.016$). Exemplar currents are shown. Calibration: 50 pA/pF, 10 ms. ***C***, ***D***, *I–V* relationships for native currents recorded from nociceptors from wild-type (***C***, ***E***) and from e37b*/e37b (***D***, ***F***) mice in control (closed circles) and after 1 h treatment with 5 μM MG132 (open circles). $Ca_V2.2$ currents are ω-conotoxin GVIA-sensitive (***C***, ***D***) and non-$Ca_V2.2$ currents are toxin-insensitive (***E***, ***F***). ***C***, Peak average current density of $Ca_V2.2$ current in wild-type neurons (37a + e37b) was −75.1 ± 6.8 pA/pF, $n = 6$ in control and −85.8 ± 10.0 pA/pF, $n = 13$ after MG132 treatment (Student's *t* test, $p = 0.32$). ***D***, Peak average current density of $Ca_V2.2$ current in neurons from e37b only mice was −74.5 ± 6.2 pA/pF, $n = 7$ in control, and −104.5 ± 13.5 pA/pF, $n = 13$ after MG132 (Student's *t* test, $p = 0.0013$). ***E***, ***F***, Peak average current density of non-$Ca_V2.2$ currents in neurons from wild-type mice (e37a + e37b) was −44.4 ± 2.8 pA/pF in control and −70.1 ± 10.9 pA/pF after MG132 treatment (***E***), and from e37b-only-expressing mice was −52.5 ± 5.1 pA/pF in control and −81.0 ± 5.9 pA/pF after MG132 (***F***). Calibrations: 50 pA/pF, 5 ms.

## Discussion

We show that sequences unique to e37b promote ubiquitination of $Ca_V2.2$. It is likely that $Ca_V2.2$ proteins contain multiple sites of ubiquitin conjugation that involve different linkages, but e37b-dependent ubiquitination is closely correlated with reduced expression of functional $Ca_V2.2$ channels and sensitivity to the ubiquitin proteasome system.

Ubiquitin covalently attaches to intracellular lysines of target proteins and depending on the type of conjugate, monoubiquitination or polyubiquitination, it can promote internalization, modify protein function, or target protein for degradation via the UPS (DiAntonio and Hicke, 2004; Macgurn et al., 2012). It is likely that the Ub-$Ca_V2.2$ signal represents a combinatorial mix of different types of ubiquitin conjugates but because of its large size (~260 kDa) relative to ubiquitin (8.5 kDa), it is not possible to draw conclusions from the position and pattern of the Ub-$Ca_V2.2$ signal in Western blots. As shown in Figures 1–3, and recently by others studying $Ca_V1.2$ and $Ca_V2.2$ (Altier et al., 2011; Waithe et al., 2011), the Ub-$Ca_V2.2$ signal is diffuse and spans a wide size range. $Ca_v2.2$ was recently identified as a target of ubiquitin based on a large-scale proteomics analysis of diGly-modified lysine residues of proteins expressed in the HCT116 cell line (Kim et al., 2011). Only one of three modified lysines identified in this screen is predicted to be intracellular, in the III-IV linker, and may be a candidate site of ubiquitin conjugation to $Ca_v2.2$ independent of e37b.

E37b-dependent ubiquitination of $Ca_V2.2$ does not necessarily occur within the e37b sequence although it is notable that lysines, K1751 and K1762, in e37b are absent in e37a (Fig. 1*A*). An overlapping region in the C terminus of $Ca_V2.2$ and a homologous region of $Ca_V1.2$ was shown recently to be critical in retaining proteins in the endoplasmic reticulum, preventing their trafficking to the plasma membrane (Altier et al., 2011). Therefore, the proximal region of the C terminus of $Ca_V2.2$ and particularly e37, commands a unique role in regulating channel expression levels.

$Ca_V\beta$ subunits are critical for trafficking $Ca_V2.2$ and $Ca_V1.2$ channels to the cell surface, and recent evidence suggests that part of their role is to protect $Ca_V2.2$ and $Ca_V1.2$ channel proteins from ubiquitin-dependent degradation by the UPS (Altier et al., 2011; Waithe et al., 2011). Consistent with these reports, we observed reduced levels of bulk $Ca_V2.2$ protein as well as Ub-$Ca_V2.2$ protein in the absence of $Ca_V\beta$. It would be interesting to test the possibility that sequences unique to e37b destabilize the $Ca_V2.2$/$Ca_V\beta_3$ subunit interaction thereby leading increased ubiquitination and degradation by the UPS.

It is striking that mutating Y1747 to F1747 in e37a not only reduces $Ca_V2.2$ current densities but also abolished $G_{i/o}$-mediated voltage-independent inhibition of $Ca_V2.2$ channels (Raingo et al., 2007). This raises the possibility that e37b-dependent ubiquitination of $Ca_V2.2$ and $G_{i/o}$-mediated voltage-independent inhibition of

$Ca_V2.2$ might converge on a common mechanism. Others have shown that activated G-protein-coupled receptors can induce ubiquitination of ion channel substrate proteins through signaling-induced E3 Ub ligase binding sites (Shukla et al., 2010).

Monitoring functional channels in addition to assessing their biochemical properties was essential because inhibition of the UPS, while substantially increasing Ub-$Ca_V2.2$ signals, did not change bulk $Ca_V2.2$ protein levels. The lack of effect of MG132 on bulk $Ca_V2.2$ protein levels at first appears incongruent with our functional studies, but this apparently paradoxical finding is typical particularly for proteins with relatively longer half lives. Results by Waithe et al., (2011, see their supplemental data) studying $Ca_V2.2$ and Altier et al. (2011) studying $Ca_V1.2$ match our findings. Similarly, in their analysis of the ubiquitinome by quantitative proteomics, Gygi and colleagues observe dramatic increases in ubiquitination events in the absence of changes in protein abundance (Kim et al., 2011). Our data showing that e37b-containing $Ca_V2.2$ channels are disproportionately affected by UPS inhibition are consistent with low stoichiometric posttranslational modifications having large effects on protein function (Kim et al., 2011).

Several groups studying both invertebrate and vertebrate preparations have shown that UPS inhibition leads to increases in synaptic efficacy through substantial presynaptic involvement (Speese et al., 2003; Bingol and Schuman, 2005; Rinetti and Schweizer, 2010). Acute inhibition of the UPS can also enhance neurotransmission in mammalian neurons, suggesting that presynaptic proteins and synaptic transmission are dynamically influenced by ubiquitination (Rinetti and Schweizer, 2010). Our findings suggest that $Ca_V2.2$ and potentially other $Ca_V2$ channels are important potential targets of inhibitors of the UPS. We show that $Ca_V2.2$ current density increases ~40% when the UPS is inhibited, a change that could alter the efficacy of excitation-secretion coupling given the steep relationship between presynaptic calcium entry and transmitter release (Bollmann et al., 2000; Schneggenburger and Neher, 2000, 2005). A similar change in the density of postsynaptic AMPA and NMDA receptors mediated by ubiquitination has a marked effect on neuronal morphology and synaptic plasticity (Colledge et al., 2003; Speese et al., 2003).

E37b-containing mRNAs represent the major pool of $Ca_V2.2$ mRNAs expressed throughout the nervous system; therefore, our findings suggest that $Ca_V2.2$ channels in most neurons are under tonic control by the UPS. In some cells, including nociceptors, cell-specific selection of e37a over e37b during alternative pre-mRNA splicing protects $Ca_V2.2$ channels from ubiquitination, suggesting some advantage for pain processing.

## References


Abramoff MD, Magalhaes PJ, Ram SJ (2004) Image processing with ImageJ. Biophotonics Int 11:36–42.

Altier C, Dale CS, Kisilevsky AE, Chapman K, Castiglioni AJ, Matthews EA, Evans RM, Dickenson AH, Lipscombe D, Vergnolle N, Zamponi GW (2007) Differential role of N-type calcium channel splice isoforms in pain. J Neurosci 27:6363–6373.

Altier C, Garcia-Caballero A, Simms B, You H, Chen L, Walcher J, Tedford HW, Hermosilla T, Zamponi GW (2011) The Cavbeta subunit prevents RFP2-mediated ubiquitination and proteasomal degradation of L-type channels. Nat Neurosci 14:173–180.

Andrade A, Denome S, Jiang YQ, Marangoudakis S, Lipscombe D (2010) Opioid inhibition of N-type $Ca^{2+}$ channels and spinal analgesia couple to alternative splicing. Nat Neurosci 13:1249–1256.

Bell TJ, Thaler C, Castiglioni AJ, Helton TD, Lipscombe D (2004) Cell-specific alternative splicing increases calcium channel current density in the pain pathway. Neuron 41:127–138.

Bingol B, Schuman EM (2005) Synaptic protein degradation by the ubiquitin proteasome system. Curr Opin Neurobiol 15:536–541.

Bloom J, Pagano M (2005) Experimental tests to definitively determine ubiquitylation of a substrate. Methods Enzymol 399:249–266.

Bollmann JH, Sakmann B, Borst JG (2000) Calcium sensitivity of glutamate release in a calyx-type terminal. Science 289:953–957.

Castiglioni AJ, Raingo J, Lipscombe D (2006) Alternative splicing in the C-terminus of CaV2.2 controls expression and gating of N-type calcium channels. J Physiol 576:119–134.

Catterall WA (2000) Structure and regulation of voltage-gated $Ca^{2+}$ channels. Annu Rev Cell Dev Biol 16:521–555.

Chen BS, Roche KW (2007) Regulation of NMDA receptors by phosphorylation. Neuropharmacology 53:362–368.

Colledge M, Snyder EM, Crozier RA, Soderling JA, Jin Y, Langeberg LK, Lu H, Bear MF, Scott JD (2003) Ubiquitination regulates PSD-95 degradation and AMPA receptor surface expression. Neuron 40:595–607.

DiAntonio A, Hicke L (2004) Ubiquitin-dependent regulation of the synapse. Annu Rev Neurosci 27:223–246.

Dolphin AC (2003) G protein modulation of voltage-gated calcium channels. Pharmacol Rev 55:607–627.

Dunlap K, Fischbach GD (1978) Neurotransmitters decrease the calcium component of sensory neurone action potentials. Nature 276:837–839.

Hille B, Beech DJ, Bernheim L, Mathie A, Shapiro MS, Wollmuth LP (1995) Multiple G-protein-coupled pathways inhibit N-type Ca channels of neurons. Life Sci 56:989–992.

Holz GG 4th, Rane SG, Dunlap K (1986) GTP-binding proteins mediate transmitter inhibition of voltage-dependent calcium channels. Nature 319:670–672.

Ikeda SR, Dunlap K (1999) Voltage-dependent modulation of N-type calcium channels: role of G protein subunits. Adv Second Messenger Phosphoprotein Res 33:131–151.

Kim W, Bennett EJ, Huttlin EL, Guo A, Li J, Possemato A, Sowa ME, Rad R, Rush J, Comb MJ, Harper JW, Gygi SP (2011) Systematic and quantitative assessment of the ubiquitin-modified proteome. Mol Cell 44:325–340.

Leroy J, Richards MW, Butcher AJ, Nieto-Rostro M, Pratt WS, Davies A, Dolphin AC (2005) Interaction via a key tryptophan in the I-II linker of N-type calcium channels is required for $\beta$1 but not for palmitoylated $\beta$2, implicating an additional binding site in the regulation of channel voltage-dependent properties. J Neurosci 25:6984–6996.

Liao P, Soong TW (2010) CaV1.2 channelopathies: from arrhythmias to autism, bipolar disorder, and immunodeficiency. Pflugers Arch 460:353–359.

Lipscombe D (2005) Neuronal proteins custom designed by alternative splicing. Curr Opin Neurobiol 15:358–363.

Macgurn JA, Hsu PC, Emr SD (2012) Ubiquitin and membrane protein turnover: from cradle to grave. Annu Rev Biochem 81:231–259.

Maximov A, Bezprozvanny I (2002) Synaptic targeting of N-type calcium channels in hippocampal neurons. J Neurosci 22:6939–6952.

Patrick GN, Bingol B, Weld HA, Schuman EM (2003) Ubiquitin-mediated proteasome activity is required for agonist-induced endocytosis of GluRs. Curr Biol 13:2073–2081.

Raingo J, Castiglioni AJ, Lipscombe D (2007) Alternative splicing controls G protein-dependent inhibition of N-type calcium channels in nociceptors. Nat Neurosci 10:285–292.

Rinetti GV, Schweizer FE (2010) Ubiquitination acutely regulates presynaptic neurotransmitter release in mammalian neurons. J Neurosci 30:3157–3166.

Rotin D, Staub O (2011) Role of the ubiquitin system in regulating ion transport. Pflugers Arch 461:1–21.

Schneggenburger R, Neher E (2000) Intracellular calcium dependence of transmitter release rates at a fast central synapse. Nature 406:889–893.

Schneggenburger R, Neher E (2005) Presynaptic calcium and control of vesicle fusion. Curr Opin Neurobiol 15:266–274.

Shukla AK, Kim J, Ahn S, Xiao K, Shenoy SK, Liedtke W, Lefkowitz RJ (2010) Arresting a transient receptor potential (TRP) channel: beta-arrestin 1 mediates ubiquitination and functional down-regulation of TRPV4. J Biol Chem 285:30115–30125.

Speese SD, Trotta N, Rodesch CK, Aravamudan B, Broadie K (2003) The ubiquitin proteasome system acutely regulates presynaptic protein turnover and synaptic efficacy. Curr Biol 13:899–910.

Waithe D, Ferron L, Page KM, Chaggar K, Dolphin AC (2011) Beta-subunits promote the expression of Ca(V)2.2 channels by reducing their proteasomal degradation. J Biol Chem 286:9598–9611.

Yi JJ, Ehlers MD (2007) Emerging roles for ubiquitin and protein degradation in neuronal function. Pharmacol Rev 59:14–39.